REGULAR PAPER

DOI: 10.1007/s40684-018-0008-7
ISSN 2288-6206 (Print) / 2198-0810 (Online)

Modified Power Prediction Model Based on Infinitesimal Cutting Force during Face Milling Process

Xiaona Luan[1,2], Song Zhang[1,2,#], and Gang Li[1,2]

1 School of Mechanical Engineering, Shandong University, Jinan, 250061, China
2 Key Laboratory of High-Efficiency and Clean Mechanical Manufacture (Minisrty of Education), Shandong University, Jinan, 250061, China
Corresponding Author / E-mail: zhangsong@sdu.edu.cn, TEL: +86-88392746

KEYWORDS: Infinitesimal cutting force, Metal removal process, Power prediction model

Nowadays soaring energy price, increasing environmental concerns, and stringent legislations make energy saving very emergency and helpful both for enterprises and environment. To deal with these issues, this paper presents a generalized mathematical power prediction model of face milling process used in manufacturing. An attempt was made to develop a relatively precise and direct power consumption model to help researchers make power optimization much easier and more practical than before. First, an infinitesimal cutting force model was proposed based on theoretical and experimental foundations. Secondly, relationship between power consumption and cutting force components was revealed, and power consumption based on infinitesimal cutting forces during metal removal process was developed. Finally, the proposed model was experimentally verified by comparing predicted and measured power consumption. Both average and instantaneous values of power consumption were used to analyze prediction error of the model. This proposed model can be used to evaluate and optimize cutting power consumption once cutting parameters were decided based on minimal energy demand. Results showed that the mean errors of maximum power and mean power were 0.076% and 0.208%, respectively. Otherwise, this proposed model will drive the field of power consumption simulation development.

Manuscript received: July 29, 2016 / Revised: May 8, 2017 / Accepted: June 13, 2017

NOMENCLATURE

dA = Cutting area of infinitesimal cutting edge (mm^2)
db = Width of cutting edge element (mm)
d_z = Thickness of infinitesimal cutting edge (mm)
dF_c = Cutting force component normal to the tool rake (N)
dF_t = Cutting force component tangential to the elementary cutting edge (N)
dF_n = Radial cutting force component (N)
F_v = Cutting force component along cutting speed v_c (N)
f_z = Feed per tooth of the milling parameters (mm/tooth)
K_{tc}, K_{nc}, K_{cc} = Cutting force coefficients (N/mm^2)
K_{te}, K_{ne}, K_{ce} = Edge force coefficients (N/mm)
$P_{a\text{-}f}$ = Additional power loss of feed drive system in cutting state (W)
$P_{a\text{-}n}$ = Additional power loss of main drive system in cutting state (W)
P_c = Total cutting power consumption of experiment (W)
$P_{c\text{-}idle}$ = Spindle motor's power consumption of the auxiliary components in cutting state (W)
P_{idle} = Spindle motor's power consumption of the auxiliary components in idling state (W)
P_{servo} = Feed motion power consumption in cutting state (W)
$P_{spindle}$ = Total spindle rotational power in cutting state (W)
P_{remove} = Total power consumption of material removing process (W)
P_u = Unload power of servo motor in feed motion system in stand-by state (W)
r = The radius of face miller (mm)
t_0 = Chip thickness (mm)
v_c = Cutting speed (m/min)
v_f = Feeding speed (m/min)
η = Additional load loss coefficient of spindle system
$\varphi(t)$ = The instantaneous cutting angle (°)
φ_{st} = Cutter entry angle (°)
φ_{ex} = Cutter exit angle (°)

1. Introduction

Traditionally, machining processes are usually optimized in order to minimize production cost. Given the increasing concern on environmental issues, especially energy consumption and the associated carbon footprints, it is possible to minimize environmental impacts of machining process by selecting cutting parameters. An accurate power prediction model which combines cutting parameters with the power consumption will accelerate the pace of this research.

In the past decades, significant research and development efforts have been made to 'green manufacturing' operations.[1] Machining processes are among the most important manufacturing activities, widely used in automotive, aerospace, and defense industries. Similar to other major manufacturing activities, machining processes carry significant environmental impacts and occupational health risks.[2] For a typical machining process, in addition to the workpiece, which is converted to an intermediate or finished part after machining, electricity consumption occupied a large portion of the inputs.[3] Electricity consumption is equal to power multiplied by time, so power consumption becomes an important factor to optimize the machining process for a minimal energy consumption objective.

Previous research about empirical power consumption model were almost based on experiments which always cost much time and material, or from the aspect of machining system which can't provide high prediction accuracy and is complicated with many factors.[4] Jang, D. et al.[5,7] developed a specific cutting energy model to optimize cutting conditions. Previous research[2,5] proved that it is necessary to divide the power consumption during a typical machining operation into some specific components to simplify power consumption model. In general, there are usually three parts, i.e., basic power, idle power, and cutting power. The power of material removal process is the actual power used to remove material. There are good theoretical computations available for cutting energy, but they are difficult to perform due to the difficulties in the calculation of all the parameters involved in the theoretical formulas.[6,7]

On the basis of machining theory, many researchers put forward various power consumption models. Li and Kara studied the relationship of P and MRR (material removal rate),[8] which was formulated as follows:

$$P = A \cdot MRR + B \tag{1}$$

Eq. (1) showed that P depended linearly on MRR, but it ignored the effect of different cutting parameters' combination at constant MRR. Two years later, Li et al. put up an improved power consumption model based on Eq. (1),[9] which was expressed thus:

$$P = \mathrm{A} \cdot MRR + \mathrm{B} \cdot n + \mathrm{C} \tag{2}$$

This improved model of Eq. (2) considered the effect of spindle speed to power consumption but still didn't analyze the effect of different cutting parameters' combination at constant MRR. Recently, Liu, N. et al. gave a cutting power model based on cutting force:[10]

$$P = \mathrm{A} + \mathrm{B} \cdot \overline{P_{cutting}} \tag{3}$$

Eq. (3) revealed that different combinations of cutting parameters at constant MRR would result different power consumption. But in the reference, calculation of $\overline{P_{cutting}}$ (average cutting power at the tool tip) was larger than P_{gap} (power gap between normal cut and air cut) which contradicted with the working principle of a machine tool. And it didn't explain why this phenomenon occurred.

Face milling and peripheral milling are two major classes of milling process. Face milling is used to cut flat surfaces (faces) into the workpiece, or to cut flat-bottomed cavities. In peripheral milling, the cutting action occurs primarily along the circumference of the cutter, so that the cross section of the milled surface ends up receiving the shape of the cutter. In this condition the blades of the cutter can be seen as scooping out material from the work piece. Face milling is widely used in the field of large-area material removing and rough machining. Infinitesimal cutting force model is proved to be more accurate than empirical formula model for a specific geometric cutter.[11] A few case studies are presented to investigate cutting force model of milling cutter with straight cutting edges,[12] ball end milling cutter,[13,14] and cylindrical milling cutter.[15,16] Investigation of face milling force based on infinitesimal cutting force has been carried out by only a few researchers.[17] Research of face milling forces were almost concentrated on its effect on surface roughness, optimization of cutting parameters and tool wear.[18,19] Research of using infinitesimal cutting forces theory to build up power prediction model has just started.[10]

An accurate power prediction model is needed to monitor the machining process to obtain minimum energy consumption and process efficiency. This research will help to elucidate the optimization and sustainability of machining processes and to underpin the reduction of electrical energy demand and carbon footprints. The purpose of this research was to propose an improved power prediction model during metal removal process based on infinitesimal cutting force. This model was function of cutting parameters for a specific couple of cutter-workpiece. Thus, once cutting parameters were decided, power consumption was acquired.

The work presented in this paper was motivated by the following observations. First, characteristics of cutting forces during metal removal process were analyzed based on the classic theory of machining. And then the infinitesimal cutting force model was built up from the aspect of mechanical dynamics. Secondly, power consumption during metal removal process P_{c} was divided into three parts to model respectively: spindle rotational power P_{spindle}, feed motion power P_{servo} and idle power $P_{\mathrm{c\text{-}idle}}$. They were all modeled based on the proposed infinitesimal cutting force model. Finally, experiment-I and experiment-II were conducted to calculate the coefficients of the proposed model and verify accuracy of the power prediction model. Comparison of the predicted data and experimental data showed that the accuracy of proposed power prediction model was reached to 99.924%. The main conclusions of this study were summarized in section "Conclusion".

2. Modeling of Cutting Forces Based on Infinitesimal Method

During a cutting process, cutting forces are very complicated and have relationship with cutter geometry, cutting conditions, and

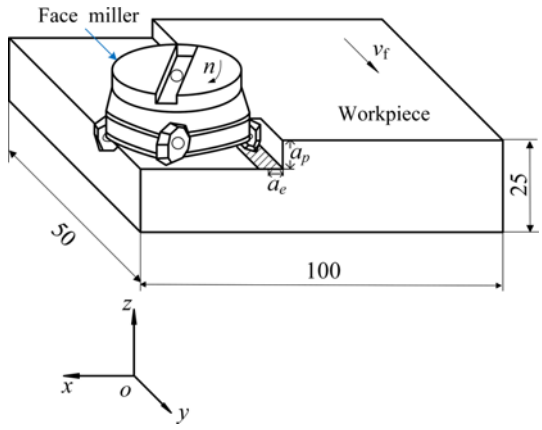

Fig. 1 Schematic diagram of face milling process

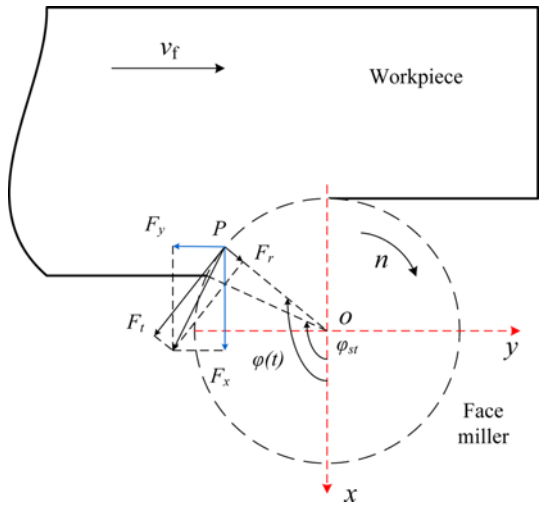

Fig. 2 Cutting force components in face milling operation

workpiece material. In this section, a face cutting force model will be presented for an inserted milling cutter under dry condition. Some assumptions will be used, which are:

(1) the cutting force component normal to the tool rank is proportional to the cutting area.[20]

(2) the radial cutting force component is proportional to the tangential cutting force.[21]

(3) the change of chip thickness is uniform and can be expressed by cutting parameters and geometrical parameters of face milling cutter.[21]

(4) the inserts have zero nose radius and zero approach angle on the inserts, and the axial components of the cutting forces become zero.[20]

2.1 Geometrical Model of Face Milling

Fig. 1 geometrically showed a face milling operation (down milling) and coordinate system of axes. As shown in Fig. 2, the chip thickness became from thick to thin during the down milling process,[22] which can be calculated form Eq. (4):

$$t_0 = t_1 \sin\alpha = f_z \sin\varphi(t) \cdot \sin\alpha \tag{4}$$

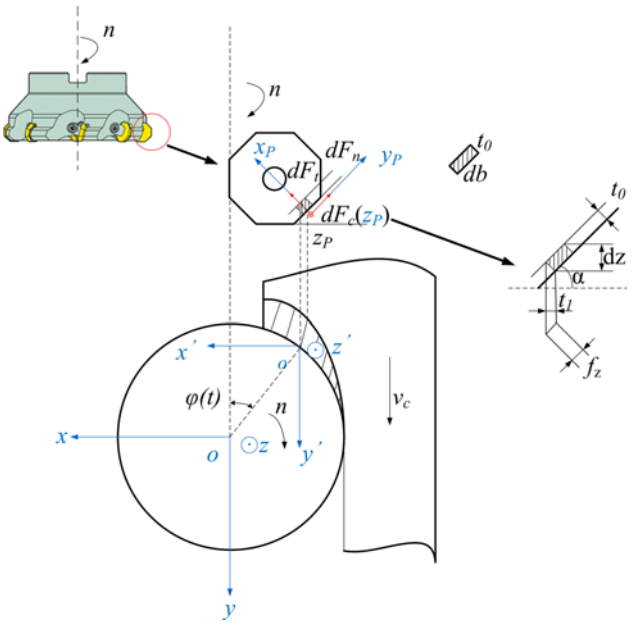

Fig. 3 Cutting force model for a milling tooth element

where, $\varphi(t)$ is the instantaneous cutting angle, which is a function of cutting parameters and geometrical relationship of cutter and workpiece.

$$\varphi(t) = \frac{\pi}{2} + \arcsin((r - a_e)/r) \tag{5}$$

where r is dynamic radius of face miller, a_e is radial depth of cut.

It must be noted that the cutting forces are produced only when the cutting tool is in the cutting zone, that is $\varphi_{st} \le \varphi(t) \le \varphi_{ex}$, where φ_{st} and φ_{ex} are the cutter entry and exit angles, respectively.

2.2. Mechanistic Force Model

The instantaneous dynamic radius on every cutting position affects the cutting forces directly since the simulated forces are proportional to chip thickness, and the chip thickness is a function of dynamic radii and feedrate. As shown in Fig. 3, dynamic radii caused by cutter run out and tilt are as follows:[23]

$$r(t) = \frac{D}{2} + r_0 = \frac{D}{2} + l\cos\alpha - d_z \cot\alpha + t_0 \tag{6}$$

where, l is length of cutting edge. dz is thickness of infinitesimal cutting edge, and $dz = a_p/N_t$, D is radius of face milling cutter.

During face milling process with inserted milling cutter, the helix angle is considered to be zero. For a point on the (j^{th}) cutting edge, differential cutting forces corresponding to an infinitesimal element thickness (d_z), which are cutting force component normal to the tool rake dF_c, tangential to the elementary cutting edge dF_t, and radial cutting force component dF_n, can be given as:[24]

$$\begin{cases} dF_t(j) = K_{te}dA + K_{te}ds \\ dF_n(j) = K_{ne}dA + K_{ne}ds \\ dF_c(j) = K_{ce}dA + K_{ce}ds \end{cases} \tag{7}$$

where, subscripts (c) and (e) represent cutting force and edge force coefficients, respectively. dA is cutting area of infinitesimal cutting

edge in mm^2, which can be expressed dA= t_0db. db is width of cutting edge in mm, while ds is the length of it in mm. From Fig. 3, db = dz/sinα. Then cutting force components are expressed as follows:

$$\begin{cases} \mathrm{d}F_{\mathrm{t}}(\mathrm{j}) = (K_{\mathrm{tc}}\dfrac{t_0}{\sin\alpha} + K_{\mathrm{te}}\dfrac{1}{\sin\alpha})\mathrm{d}z \\ \mathrm{d}F_{\mathrm{n}}(\mathrm{j}) = (K_{\mathrm{nc}}\dfrac{t_0}{\sin\alpha} + K_{\mathrm{ne}}\dfrac{1}{\sin\alpha})\mathrm{d}z \\ \mathrm{d}F_{\mathrm{c}}(\mathrm{j}) = (K_{\mathrm{cc}}\dfrac{t_0}{\sin\alpha} + K_{\mathrm{ce}}\dfrac{1}{\sin\alpha})\mathrm{d}z \end{cases} \tag{8}$$

In Fig. 3, three coordinate systems are defined to realize the change of cutting forces from cutting-tool system to workpiece system. Once the infinitesimal component forces dF_{t}, dF_{n}, dF_{c} on the cutting edge are determined, cutting forces in the coordinate system of $ox'y'z'$ can be expressed through the following transformation:

$$\begin{bmatrix} \mathrm{d}F_{x'(\mathrm{j})} \\ \mathrm{d}F_{y'(\mathrm{j})} \\ \mathrm{d}F_{z'(\mathrm{j})} \end{bmatrix} = M_1 \begin{bmatrix} \mathrm{d}F_{\mathrm{t(j)}} \\ \mathrm{d}F_{\mathrm{n(j)}} \\ \mathrm{d}F_{\mathrm{c(j)}} \end{bmatrix} \tag{9}$$

where, $M_1 = \begin{bmatrix} \sin\alpha & -\cos\alpha & 0 \\ 0 & 0 & -1 \\ \cos\alpha & \sin\alpha & 0 \end{bmatrix}$, and transition matrix of $ox'y'z'$ to $oxyz$ is as follows,

$$M_2 = \begin{bmatrix} -\cos\varphi(\mathrm{t}) & 0 & 0 \\ 0 & -\cos\varphi(\mathrm{t}) & 0 \\ 0 & 0 & 1 \end{bmatrix}.$$

and then transition matrix of $ox_Py_Pz_P \rightarrow oxyz$ is equal to M_2 multiplied by M_1, $M = M_2 \cdot M_1$.

Finally, cutting force components in machine tool coordinate system is acquired by the following transformation:

$$\begin{bmatrix} \mathrm{d}F_{x(\mathrm{j})} \\ \mathrm{d}F_{y(\mathrm{j})} \\ \mathrm{d}F_{z(\mathrm{j})} \end{bmatrix} = M \cdot \begin{bmatrix} \mathrm{d}F_{\mathrm{t(j)}} \\ \mathrm{d}F_{\mathrm{n(j)}} \\ \mathrm{d}F_{\mathrm{c(j)}} \end{bmatrix} \tag{10}$$

where, $M = \begin{bmatrix} -\sin\alpha\cos\varphi(\mathrm{t}) & \cos\alpha\cos\varphi(\mathrm{t}) & \sin\varphi(\mathrm{t}) \\ \sin\alpha\cos\varphi(\mathrm{t}) & -\cos\alpha\sin\varphi(\mathrm{t}) & \cos\varphi(\mathrm{t}) \\ \cos\alpha & \sin\alpha & 0 \end{bmatrix}$.

The resulting cutting forces for one cutting edge F_{x}, F_{y}, and F_{z} can be calculated from the infinitesimal component forces dF_{x}, dF_{y}, and dF_{z} as shown in Eq. (11).

$$\begin{cases} F_x = \sum_{\mathrm{j}=1}^{N_t} \mathrm{d}F_{x(\mathrm{j})} = \sum_{\mathrm{j}=1}^{N_t} (-\sin\alpha\cos\varphi(\mathrm{t})\mathrm{d}F_{\mathrm{t(j)}} - \cos\alpha\cos\varphi(\mathrm{t})\mathrm{d}F_{\mathrm{n(j)}} + \sin\varphi(\mathrm{t})\mathrm{d}F_{\mathrm{c(j)}}) \\ F_y = \sum_{\mathrm{j}=1}^{N_t} \mathrm{d}F_{y(\mathrm{j})} = \sum_{\mathrm{j}=1}^{N_t} (\sin\alpha\sin\varphi(\mathrm{t})\mathrm{d}F_{\mathrm{t(j)}} - \cos\alpha\sin\varphi(\mathrm{t})\mathrm{d}F_{\mathrm{n(j)}} + \cos\varphi(\mathrm{t})\mathrm{d}F_{\mathrm{c(j)}}) \\ F_z = \sum_{\mathrm{j}=1}^{N_t} \mathrm{d}F_{z(\mathrm{j})} = \sum_{\mathrm{j}=1}^{N_t} (\cos\alpha\mathrm{d}F_{\mathrm{t(j)}} + \sin\alpha\mathrm{d}F_{\mathrm{n(j)}}) \end{cases} \tag{11}$$

2.3 Calculation of Force Coefficients

In mechanistic approach, the total cutting forces are proportional to cutting force coefficients K_{tc}, K_{nc}, K_{cc} and edge force coefficients K_{te}, K_{ne}, K_{ce}, which can be calculated by a set of experiments.[25,26]

Budak, E. et al. gave a method of mechanistic evaluating the cutting force coefficients.[21] Some research indicated that the exponential force model could be integrated into liner force model which contains the six coefficients. A mechanistic method of calibrating the milling tools is put forward which is also suitable for face miller.[21] A set of milling experiments are conducted at different feed rates, but at constant immersion and axial depth of cut. The cutting forces are measured by specific dynamometer.

The instantaneous cutting forces per spindle revolution were collected for many periods and divided by the rotation period to decreases the measurement error. Besides, if there is more than one cutting tooth simultaneously depending on the number of teeth on the cutter (N) and the radial width of cut. In this condition, the cutter pitch angle is given as follows:

$$\varphi_{\mathrm{p}} = 2\pi/N \tag{12}$$

The average cutting forces are independent of helix angle, owing to that the total material removed per tooth period is constant with or without helix angle. Then the average cutting forces per tooth period can be expressed by integrating the instantaneous cutting force $F_{\mathrm{q}}(\varphi)$ in one revolution and dividing by the pitch angle as follows:

$$\bar{F}_{\mathrm{q}} = \frac{1}{\varphi_{\mathrm{p}}} \int_{\varphi_{\mathrm{st}}}^{\varphi_{\mathrm{ex}}} F_{\mathrm{q}}(\varphi) d\varphi \tag{13}$$

where, $q = x, y, z$.

The total cutting forces are separated into two parts. The edge force F_{qe} represents the parasitic part of the forces which are not due to cutting, and thus do not depend on the uncut chip thickness, whereas the cutting forces F_{qc} (q= x, y, z) do. The average cutting forces can be expressed by a linear function of feed rate f_{z} and an offset contributed by the edge forces as follows:

$$\bar{F}_{\mathrm{q}} = \bar{F}_{\mathrm{qc}} \cdot f_{\mathrm{z}} + \bar{F}_{\mathrm{qe}} \tag{14}$$

The cutting edge components (F_{qc}, F_{qe}) were estimated from the measured average forces at each feed rate by a mathematical method of linear regression. Experimental data of cutting forces were used for doing this procedure to resolve the (F_{qc}, F_{qe}).

$$\begin{aligned} \vec{F}_{\mathrm{x}} &= \vec{F}_{\mathrm{xc}} \cdot f_{\mathrm{z}} + \vec{F}_{\mathrm{xe}} \\ \vec{F}_{\mathrm{y}} &= \vec{F}_{\mathrm{yc}} \cdot f_{\mathrm{z}} + \vec{F}_{\mathrm{ye}} \\ \vec{F}_{\mathrm{z}} &= \vec{F}_{\mathrm{zc}} \cdot f_{\mathrm{z}} + \vec{F}_{\mathrm{ze}} \end{aligned} \tag{15}$$

Linear regression uses the least square method to fit the measured data. Experiments for significance of regression and individual model coefficients were performed to verify goodness of fit for the model.

Finally, the cutting force coefficients for the linear-edge force model are evaluated from Eqs. (15) and (16) as follows:[27]

$$\begin{aligned} &K_{\mathrm{tc}} = 4\frac{\bar{F}_{\mathrm{xc}}P + \bar{F}_{\mathrm{yc}}Q}{P^2+Q^2},\ K_{\mathrm{nc}} = \frac{K_{\mathrm{tc}}P - 4\bar{F}_{\mathrm{xc}}}{Q},\ K_{\mathrm{cc}} = \frac{\bar{F}_{\mathrm{zc}}}{T}, \\ &K_{\mathrm{te}} = \frac{\bar{F}_{\mathrm{xc}}S + \bar{F}_{\mathrm{xc}}T}{S^2+T^2},\ K_{\mathrm{ne}} = \frac{K_{\mathrm{te}}S + \bar{F}_{\mathrm{ye}}}{T},\ K_{\mathrm{ce}} = -\frac{2\pi}{aN}\frac{\bar{F}_{\mathrm{ze}}}{\varphi_{\mathrm{ex}} - \varphi_{\mathrm{st}}} \end{aligned} \tag{16}$$

where, $P = \frac{aN}{2\pi}[\cos 2\varphi]_{\varphi_{\mathrm{st}}}^{\varphi_{\mathrm{ex}}}$, $\mathrm{T} = \frac{aN}{2\pi}[\cos\varphi]_{\varphi_{\mathrm{st}}}^{\varphi_{\mathrm{ex}}}$, $S = \frac{aN}{2\pi}[\sin\varphi]_{\varphi_{\mathrm{st}}}^{\varphi_{\mathrm{ex}}}$, $Q = \frac{aN}{2\pi}[2\varphi$

$-\sin 2\varphi]_{\varphi_{st}}^{\varphi_{ex}}$, and $(\bar{F}_{qc}, \bar{F}_{qe})$ $(q = x, y, z)$ are components of edge forces.

After the above procedures have all been done, the proposed cutting force model can be expressed by taking the coefficients K_{tc}, K_{nc}, K_{cc}, K_{te}, K_{ne}, and K_{ce} into Eq. (11) combing with Eqs. (8) and (9). This procedure is repeated for different cutter geometry, and also can be used for predicting cutter constants before cutter is manufactured.

3. Modeling of Power Consumption during Face Milling Process

For a typical machining process, power consumption model of a computer numerical control (CNC) system is really complicated and is always simplified and classified into two parts in convenience of modeling: the material removing power consumption P_{remove} which is caused by removing material and the idle power consumption $P_{c\text{-}idle}$ which is caused by auxiliary equipment during idle process. These power consumption components models were built up respectively.

3.1 Power Characteristics of a Machine Tool during Face Milling Process

In this research, cutting power consumption especially refers to the tool movement with performing the cutting operation. During this duration, expect the material removal, the tool movement, spindle, coolant pump, etc. all consume energy. Considering feasibility and complexity of total cutting power consumption P_c modeling, P_c is divided into two components P_{remove} and $P_{c\text{-}idle}$.

P_{remove} is affected by the cutting parameters and workpiece material which have some relationship with cutting forces. Based on the theory of manufactural dynamics, material removing process is finished by spindle rotation and feed motion, which are driven by main motor and servo motors respectively. Accordingly, power consumption during material removing process P_{remove} can be calculated by adding up spindle rotation power consumption $P_{spindle}$ and servo motors power consumption P_{servo}. $P_{spindle}$ and P_{servo} can be calculated by cutting force F_i multiplied by cutting speed v_i along the direction of cutting force component.

$P_{c\text{-}idle}$ refers to the power consumption of auxiliary components in cutting state. Due to additional load in machining state, power consumption of auxiliary components $P_{c\text{-}idle}$ is different from that in idle state P_{idle}. In another word, $P_{c\text{-}idle}$ has some relationship with cutting parameters and other cutting condition.

The model of power consumption during material removal process P_c can be expressed by the following formula:

$$P_c = P_{remove} + P_{c\text{-}idle} = P_{spindle} + P_{servo} + P_{c\text{-}idle} \tag{17}$$

The modeling method of $P_{spindle}$, P_{servo} and $P_{c\text{-}idle}$ was introduced in the following sections based on the theory of infinitesimal cutting forces in section 2.

3.2 Calculation of Spindle Power Consumption $P_{spindle}$

Spindle motor provides power for main driving system of machine tools. Spindle rotational power consumption $P_{spindle}$ occupies a large component of P_{remove} and is affected by the spindle speed for a specific couple of cutter-workpiece. Spindle rotational power consumption of tool cutter point $P_{spindle}$ is equal to peripheral force F_v multiplied by cutting speed v_c.[3] For an infinitesimal cutting edge, $dP_{spindle}$ was expressed as follows:

$$dP_{spindle} = dF_v \cdot v_c = dF_v \cdot 2\pi nR \tag{18}$$

where, F_v is peripheral cutting force in N (cutting system), v_c is cutting speed in m/min, n is rotational speed of spindle in r/min, and R is radius of face milling cutter in mm.

According to the cutting force analysis in section 2.2, the peripheral cutting force F_v is equal to the cutting force component which is tangential to the elementary cutting edge F_t.

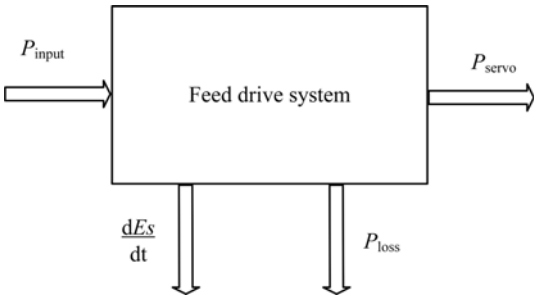

Fig. 4 Transient energy flow diagram of feed drive system

3.3 Calculation of Feed Motion Power Consumption P_{servo}

Based on the theory of interaction force, additional power of main motor caused by feed motion is equal to the feed rate v_f multiplied by the cutting force component along its direction F_t. Accordingly, the feed motion power consumption P_{servo} can be verified by the experimental measured power data of specific servo motor.

For feed drive system, its operation process can be considered as a complete energy flow during manufacturing process. Fig. 4 showed a transient energy flow diagram of feed drive system. P_{input} is the total power input into feed drive system, dEs/dt is a dynamic process of power storage or release, P_{loss} is power loss and P_{servo} is power output for removing material, which used for removing material and is defined as feed motion power in this research.

When $P_{servo} = 0$, machine tool is in a stand-by state, there is a unload power P_u of servo motor to maintain essential movement, and P_u has no relation with cutting load. Previous research revealed that P_u was a process of first decreasing gradually stable in guide way travel range,[28] so value of P_u should be recorded at stable state.

When $P_{servo} \neq 0$, feed drive system is in a machining state. Resistance of feed drive system and servo motor's magnetic are changed with different cutting load. Accordingly, the total power losses P'_u of feed drive system and servo motor increases based on power load loss P_u in stand-by state. This additional part $P_{a\text{-}f}$ is defined as additional power loss of feed drive system which can't be measured directly by power monitoring system. In cutting state,

$$P'_u = P_u + P_{a\text{-}f} \tag{19}$$

In machine tool coordinate system, cutting force component along

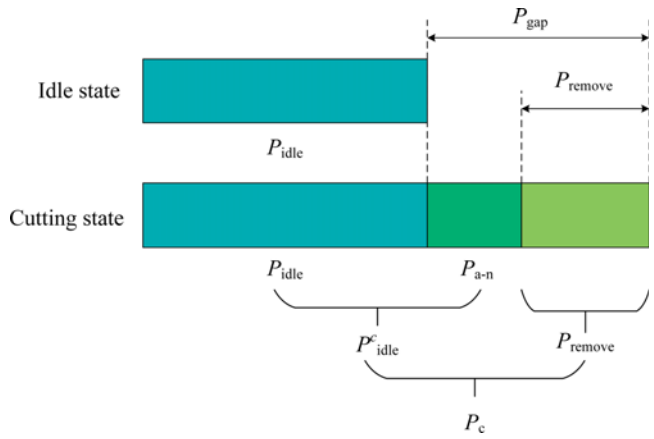

Fig. 5 Power distribution of main drive system

the feed motion direction can be measured directly by a specific dynamometer experimentally; on the other hand, it can be acquired by coordinate transformations in section 2 theoretically. Similarly, P_{servo} is calculated by the cutting force component F_t multiplied by v_f. For an infinitesimal cutting edge, dP_{servo} was expressed as follows:

$$dP_{servo} = dF_t \cdot v_f \tag{20}$$

where, dF_t is cutting force component along feed motion direction in N (machine tool coordinate system), v_f is feeding speed in m/min.

3.4 Calculation of Idle Power Consumption $P_{c\text{-}idle}$

In this research, idle power consumption P_{idle} specific refers to power consumption of main drive system in idle state, while $P_{c\text{-}idle}$ is in cutting state. P_{idle} is similar to the unload power P_u of feed motion system, which has no relation with cutting load.

When P_{remove}= 0, spindle is idling. The idle power P_{idle} has relation with spindle speed n. In a specific spindle speed, P_{idle} is a process of first decreasing gradually stable, so value of P_{idle} should also be recoded at stable state and then calculated the average.

When $P_{remove} \neq 0$, spindle is at machining state. Different cutting load will result in different additional power loss $P_{a\text{-}n}$ due to various frictions among machine tool components. In another word, power consumption of axially components in machining state $P_{c\text{-}idle}$ is a little larger than that of idle state P_{idle}. These theoretical conclusions will be verified by experimental results in following section. Thus,

$$P_{c\text{-}idle} = P_{idle} + P_{a\text{-}n} \tag{21}$$

Form the above research of main motor and servo motor, a novel conclusion and explanation was put forward. The mechanism of additional power loss revealed why the power gap P_{gap} between normal cut P_c and air cut P_{idle} is not equal to P_{remove} proposed by Liu N. et al..[10] But P_{gap} is larger than the material removal power P_{remove} (this is contradict with the viewpoint that P_{gap} is smaller than P_{remove} by Liu, N. et al.[10]), which is clearly observed in Fig. 5.

Hu S., et al. pointed out that power consumed by auxiliary systems $P_{c\text{-}idle}$ is approximately proportional to the cutting power consumption of tool cutter point $P_{spindle}$,[29] which described thus:

$$P_{c\text{-}idle} = \eta P_{spindle} \tag{22}$$

where, η is the additional load loss coefficient.

3.5 Calculation of Total Cutting Power Consumption P_c

Based on modeling of $P_{c\text{-}idle}$, $P_{spindle}$ and P_{servo}, the cutting power consumption P_c Eq. (17) can be defined thus:

$$P_c = (1+\eta)P_{spindle} + P_{servo} \tag{23}$$

Then, the cutting power consumption P_c was calculated by combining Eqs. (8), (18), (20), (22) with (17):

$$\begin{aligned} P_c &= (1+\eta)\frac{F_v v_c}{60} + F_t v_f \\ &= (1+\eta)\frac{\sum_{z=1}^{N_i}(K_{tc}\frac{t_0}{\sin\alpha} + K_{te}\frac{1}{\sin\alpha})dz \cdot 2\pi nR}{60} + F_t \cdot \eta f_z z \end{aligned} \tag{24}$$

where, F_t is instantaneous tangential component (cutter coordinate system), v_c is cutting speed, n is the spindle speed in r/min.

The investigation by Hu S., et al. showed that additional load loss coefficient η of the model in Eq. (22) is machine tool dependent variable.[29] For the machining center DAEWOO ACE-V500, η was 0.362 which could acquire from the experimental results in the simulation model. This cutting power consumption prediction model was built up based on the mechanical infinitesimal cutting force model, which can accurately illustrate the real-time power consumption change during cutting process. Besides, this model can predict the power consumption once the cutting parameters were decided and then optimize them to minimize the power consumption.

4. Experimental Details

The coefficients of the cutting forces model were calculated from cutting force data from experiment-I. Then, error analysis and experiments are usually used to modify if the proposed power consumption model could accurately predict the result or not. In this section, a series of machining experiments (experiment-II) were conducted to investigate the accuracy of the proposed model.

4.1 Design of Cutting Parameters

Based on the theory of calculating coefficients in section 2.3, a set of face milling experiments at different feeds per tooth but constant axial depth of cut and immersion have to be conducted in experiment-I. In this research, 14 tests were done to measure cutting forces which were designed as follows: v_c = 593.76 m/min, a_p = 0.5 mm, a_e = 1.85 mm, and f_z = 0.1-0.62 mm/tooth with an interval of 0.04 mm/tooth.

To verify the accuracy of the proposed power prediction model, experiments (experiment-II) were conducted with different combinations of cutting parameters, which is listed in Table 1.

4.2 Experimental Setup

In experiment-I and experiment-II, one piece of cutter (Seco F40M)

Table 1 Cutting parameters of verification experiments(experiment-II)

No.	v_c (m/min)	f_z (mm/z)	a_p (mm)	a_e (mm)
1	187.5	0.38	1.6	1.85
2	160.0	0.25	0.9	0.95
3	132.5	0.13	1.6	1.85
4	105.0	0.50	0.9	2.75
5	77.5	0.38	1.6	1.85

Table 2 Chemical composition of HTCuCrSn -250 (*wt.* %)

Ele.	C	Mn	S	P	Si	Cu	Cr	Sn	Fe
Min.	3.16	0.89	0.09	0.12	1.79	0.40	0.20	0.06	Bal.
Max.	3.30	1.04	0.13	0.17	1.93	0.60	0.35	0.08	

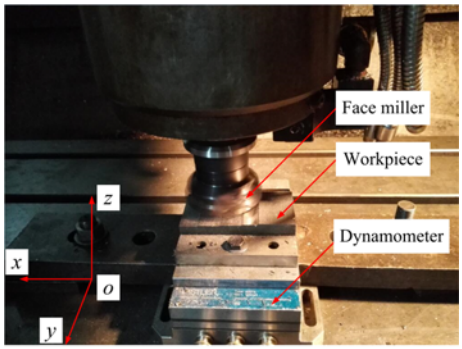

(a) Workpiece and cutting tool

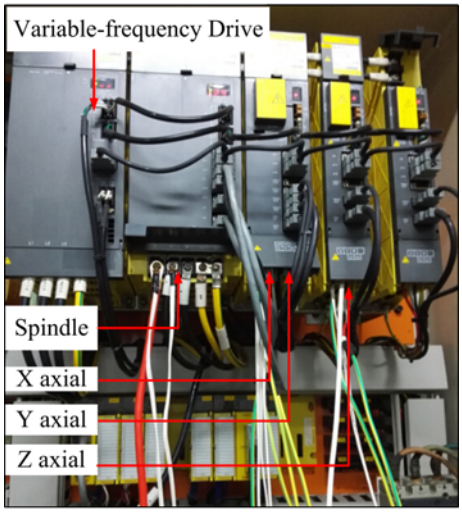

(b) Power monitoring system

Fig. 6 Experimental process of face milling

with liner-cutting edges was inserted in cutter head (Seco R220.43-0063-07W) and used for experiments. The cutter Seco F40M is coated with TiAlN and suitable for cutting alloy cast iron as recommended by the tool manufacturer Seco.

The workpiece was a diesel engine cylinder block part made of alloy cast iron- HTCuCrSn -250, which is different from the traditional HT250 because of the additional elements and the content. The chemical composition is as shown in Table 2. The workpiece used in the face milling experiments were heat-treated and annealed. It is possible to carry out a great number of experiments in a large range of cutting parameters without tool wear. Rectangular blocks of HT250 casting blank were prepared in the dimensions of 100 mm × 50 mm × 25 mm and the surface materials of workpiece were removed to get rid of the influence to the quality of processing surface.

The face milling experiments were performed on a three-axis vertical machining center DAEWOO ACE-V500 with speed range of spindle 10000 rpm. The rated power of main motor is 15 kW and servo motor's is 3.8 kW.

All the experiments were conducted in down milling process under dry cutting condition. The instantaneous cutting force components in *x*-, *y*-, and *z*- directions, F_x, F_y, and F_z were recorded by using Kistler 9257A dynamometer. Fig. 6 showed a process of face milling experiments and the geometrical details of the milling cutter. Power consumption during machining process was calculated from the variable voltage and current which measured by a NI-9220 data acquisition card.[30] As shown in Fig. 6(b), the voltage and current were measured from the output of variable-frequency drive module. In all experiments, cutting forces were measured and the six coefficients are calculated through experimental average force data.

5. Results and Discussion

5.1 Results of Coefficients and Verification of Cutting Force Model

According to the procedure introduced in the above section 2.3, coefficients of octagonal cutter were calculated combing with the experimental data as follows:

Obviously, in experiment-I, axial depth of cut was a constant a_p= 0.5 mm and the number of cutting tooth was N = 1, while cutting type was down milling, the cutting in and out angle were $\varphi_{ex} = \pi$, $\varphi_{st} = 160.27 \times \pi/180$, respectively. Then taking these data into the expression of P, Q, T, and S in section 2.3, values of them can be get P = 0.0181, Q = 0.0042, T = -0.0047, S = -0.0269.

Then, the cutting edge components (F_{qc}, F_{qe}) were calculated by liner regression of the experimental results.

$$\begin{aligned} \vec{F}_x &= \vec{F}_{xc} \cdot f_z + \vec{F}_{xe} = 139.7942 \cdot f_z + 28.0810 \\ \vec{F}_y &= \vec{F}_{yc} \cdot f_z + \vec{F}_{ye} = 141.5380 \cdot f_z + 30.2875 \\ \vec{F}_z &= \vec{F}_{zc} \cdot f_z + \vec{F}_{ze} = 93.3600 \cdot f_z + 13.1493 \end{aligned} \tag{25}$$

Then taking the cutting edge components in Eq. (25) into Eq. (16), the values of six coefficients were calculated as follows: $K_{tc} = 2.6203 \times 10^4$, $K_{nc} = 2.2879 \times 10^4$, $K_{cc} = -1.9864 \times 10^4$, $K_{te} = -1.1052 \times 10^3$, $K_{ne} = -1.277010^4$, $K_{ce} = -0.3291$, respectively. Taking these coefficients into Eq. (8), three component cutting forces in workpiece system were finally acquired. The evaluated coefficients are valid only for the specific cutter geometry tested.

Finally, simulation of the cutting force model was shown in Fig. 7. To verify the accuracy of the proposed cutting force model, the simulation results were compared with the experimental results.

The above analytical results showed that the cutting time was corresponding to the simulation result in Fig. 7, as well as the rotation period. The minor difference between the predicted value and the experimental value was shown in Fig. 7(b), Some random factors during milling process, such as, tool vibrations, stiffness of the

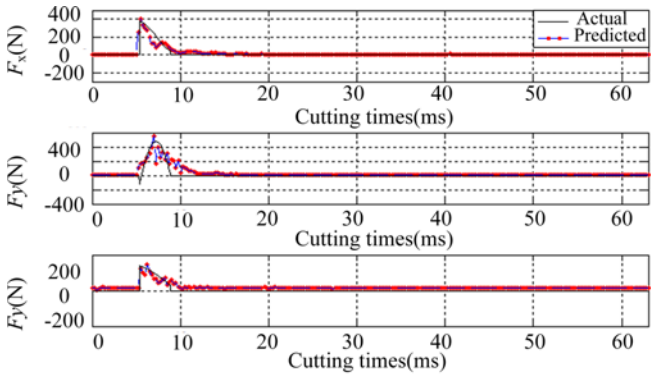

(a) Cutting forces of two cutting periods (experiment-II-1)

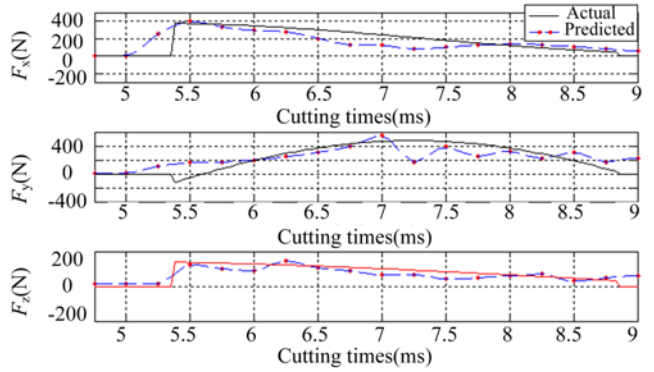

(b) Local amplification of cutting forces (experiment-II-1)

Fig. 7 Comparisons of simulation and experimental results of three cutting force components

Table 3 Comparison between predicted and actual cutting forces of experiments

No.	Predicted			Experimental data			Error_F
	F_x^*(N)	F_y^*(N)	F_z^*(N)	F_x(N)	F_y(N)	F_z(N)	(%)
1	199.64	260.38	105.35	203.58	263.53	106.02	1.25
2	166.78	213.26	90.82	168.29	215.16	91.59	0.87
3	150.31	231.65	92.49	151.07	234.87	93.11	0.84
4	162.35	196.82	138.75	163.69	196.13	139.46	0.32
5	156.23	205.34	95.38	157.12	206.04	96.34	0.63

transmission system and heterogeneity of workpiece material, can result in that the real cutting forces (experimental results) deviate from the desired values. Besides, the peak of the cutting force by experimental measured was nearly corresponding to the simulation result. To quantitatively evaluate the accuracy of the cutting force model, the mean cutting forces were analyzed for every experimental data which were listed in Table 3. From Table 3, it's obviously that the errors of the cutting force model were all lower than 2% and the mean error was 0.78%, which was in a permitted range. In a word, the theoretical cutting force model could accurately predict the cutting force.

5.2 Accuracy Analysis of Proposed Power Prediction Model

The coefficients of the power prediction model were calculated by the measured data from experiment-I. And the proposed model was finally expressed as follows:

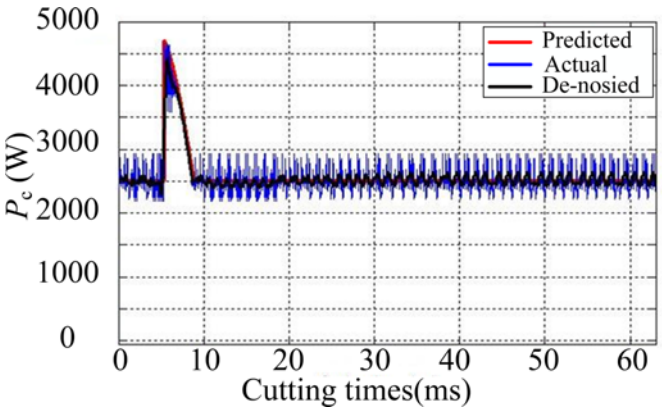

Fig. 8 Comparisons of the predicted and actual results of power consumption (experiment-II-1)

Table 4 Comparison between predicted powers and actual power readings of experiments

	P_c_max (W)	P^*_c_max (W)	Error_P^*_c (%)	$\overline{P}_c$ (W)	$\overline{P}^*_c$ (W)	Error $\overline{P}_c$ (%)
1	4586.1	4581.31	0.10	3619.3	3614.46	0.13
2	3753.3	3749.73	0.09	2931.5	2928.89	0.08
3	4354.4	4350.36	0.09	2724.9	2712.92	0.43
4	4241.2	4240.6	0.01	3024.1	3012.29	0.39
5	4084.1	4080.26	0.09	3015.7	3015.36	0.01

$$P = (1+\eta)\frac{F_t v_c}{60} + F_f v_f = (1+\eta)\frac{\sum_{z=1}^{N_i}\left(K\frac{t_0}{\sin\alpha}+K\frac{1}{\sin\alpha}\right)dz\cdot 2\pi nR}{60} + F_y\cdot nf_z \quad (26)$$

Taking Eqs. (11) and (16) into (26), the instantaneous predicted and actual cutting power curve were showed in Fig. 8. The vibration signal was de-noised by "sgolay filtering" in Matlab. From Fig. 8, it is obviously that the predicted cutting period and power changed trend were all corresponding to experimental result.

Furthermore, error analysis was conducted to verify accuracy of the proposed model. In experiment-II, measured power values for every experiment were used to determine its average $\overline{P}_c$. Both mean errors and maximum errors of power consumption were analyzed by following expression and the results were listed in Table 4,

$$Error = \frac{P_c^* - P_c}{P_c} \quad (27)$$

where, P_c^* is predicted power consumption value, P_c is experimental power consumption value.

Table 4 showed that prediction errors of the proposed model achieved lower than 0.1% and 0.5%, which were errors of maximum power and mean power, respectively. And mean errors of maximum power and mean power were 0.076% and 0.208%, respectively. The mean power prediction error was a little larger than the maximum power prediction error, which was owing to vibration and other uncertain factors during cutting process but it was ignored in the proposed model. Therefore, the proposed power prediction model has

high accuracy to predicting the cutting power consumption of the spindle motor during metal removal process.

Besides, a novel phenomenon was observed in the process of power prediction modeling. The additional feed motion power P_{servo} ($P_{servo} = F_t \times v_f$) of the spindle motor during cutting process is closely related to that of servo motor $P_{c\text{-}f}$. Further exploration of the relationship between P_{servo} and $P_{c\text{-}f}$ is still under study.

6. Conclusions

This research proposed an improved power consumption model during metal removal process based on infinitesimal cutting force theory. The power consumption during metal removal process was divided into three parts: spindle rotational power P_{remove}, feed motion power P_{servo} and idle power $P_{c\text{-}idle}$. This modeling method reduces complexity of modeling process, while improving accuracy of the prediction model comparing with previous mathematical models. Experimental data were used to verify accuracy of the proposed model. Following conclusions were summarized from this research:

(1) Power consumption of the main spindle motor during metal removal process P_c can be divided into three components based on the characteristics of the cutting movement for further study.

(2) The error of mean power (0.208%) is a little larger than the error of maximum power (0.076%), which is owing to the complex factors of the cutting process. The experimental data have some vibrations, but the prediction data change smoothly.

(3) Feed motion power P_{servo} ($P_{servo} = F_t \times v_f$) of spindle motor during cutting process is closely related to that of servo motor $P_{c\text{-}f}$.

(4) To some extent, the proposed power prediction model will push the development of power consumption simulation field.

ACKNOWLEDGEMENT

This work is supported by National Major Science and Technology Project: High-end CNC Machine Tools and Basic Manufacturing Equipments (Grant No. 2015ZX04003-005), and Taishan Scholars Program of Shandong Province.

REFERENCES

1. Campatelli, G., Scippa, A., Lorenzini, L., and Sato, R., "Optimal Workpiece Orientation to Reduce the Energy Consumption of a Milling Process," Int. J. Precis. Eng. Manuf.-Green Tech., Vol. 2, No. 1, pp. 5-13, 2015.
2. Zhao, F. and Sharma, A., "Environmentally Friendly Machining Machining Process Environmentally Friendly Machining," Handbook of Manufacturing Engineering and Technology, pp. 1127-1154, 2015.
3. Liu, F., Xie, J., and Liu, S., "A Method for Predicting the Energy Consumption of the Main Driving System of a Machine Tool in a Machining Process," Journal of Cleaner Production, Vol. 105, pp. 171-177, 2015.
4. Velchev, S., Kolev, I., Ivanov, K., and Gechevski, S., "Empirical Models for Specific Energy Consumption and Optimization of Cutting Parameters for Minimizing Energy Consumption during Turning," Journal of Cleaner Production, Vol. 80, pp. 139-149, 2014.
5. Jang, D., Jung, J., and Seok, J., "Modeling and Parameter Optimization for Cutting Energy Reduction in MQL Milling Process," Int. J. Precis. Eng. Manuf.-Green Tech., Vol. 3, No. 1, pp. 5-12, 2016.
6. Yoon, H.-S., Lee, J.-Y., Kim, M.-S., and Ahn, S.-H., "Empirical Power-Consumption Model for Material Removal in Three-Axis Milling," Journal of Cleaner Production, Vol. 78, pp. 54-62, 2014.
7. Al-Hazza, M. H. F., Adesta, E. Y. T., Ali, A. M., Agusman, D., and Suprianto, M., "Energy Cost Modeling for High Speed Hard Turning," Journal of Applied Sciences, Vol. 11, No. 14, pp. 2578-2584, 2011.
8. Li, W. and Kara, S., "An Empirical Model for Predicting Energy Consumption of Manufacturing Processes: A Case of Turning Process," Proceedings of the Institution of Mechanical Engineers, Part B: Journal of Engineering Manufacture, Vol. 225, No. 9, pp. 1636-1646, 2011.
9. Li, L., Yan, J., and Xing, Z., "Energy Requirements Evaluation of Milling Machines Based on Thermal Equilibrium and Empirical Modelling," Journal of Cleaner Production, Vol. 52, pp. 113-121, 2013.
10. Liu, N., Zhang, Y., and Lu, W., "A Hybrid Approach to Energy Consumption Modelling Based on Cutting Power: A Milling Case," Journal of Cleaner Production, Vol. 104, pp. 264-272, 2015.
11. Liu, X.-W., Cheng, K., Webb, D., and Luo, X.-C., "Prediction of Cutting Force Distribution and Its Influence on Dimensional Accuracy in Peripheral Milling," International Journal of Machine Tools and Manufacture, Vol. 42, No. 7, pp. 791-800, 2002.
12. Ehmann, K., Kapoor, S., DeVor, R., and Lazoglu, I., "Machining Process Modeling: A Review," Journal of Manufacturing Science and Engineering, Vol. 119, pp. 655-663, 1997.
13. Wei, Z., Wang, M., Zhu, J., and Gu, L., "Cutting Force Prediction in Ball End Milling of Sculptured Surface with Z-Level Contouring Tool Path," International Journal of Machine Tools and Manufacture, Vol. 51, No. 5, pp. 428-432, 2011.
14. Abou-El-Hossein, K., Kadirgama, K., Hamdi, M., and Benyounis, K., "Prediction of Cutting Force in End-Milling Operation of Modified AISI P20 Tool Steel," Journal of Materials Processing Technology, Vol. 182, No. 1, pp. 241-247, 2007.
15. Sun, Y., Ren, F., Guo, D., and Jia, Z., "Estimation and Experimental Validation of Cutting Forces in Ball-End Milling of Sculptured Surfaces," International Journal of Machine Tools and Manufacture, Vol. 49, No. 15, pp. 1238-1244, 2009.
16. Gradišek, J., Kalveram, M., and Weinert, K., "Mechanistic Identification of Specific Force coefficients for a General end Mill," International Journal of Machine Tools and Manufacture, Vol. 44, No. 4, pp. 401-414, 2004.

17. Fu, H.-J., DeVor, R., and Kapoor, S., "A Mechanistic Model for the Prediction of the Force System in Face Milling Operations," Journal of Engineering for Industry, Vol. 106, No. 1, pp. 81-88, 1984.

18. Korkut, I. and Donertas, M., "The Influence of Feed Rate and Cutting Speed on the Cutting Forces, Surface Roughness and Tool-Chip Contact Length during Face Milling," Materials & Design, Vol. 28, No. 1, pp. 308-312, 2007.

19. Baek, D. K., Ko, T. J., and Kim, H. S., "Optimization of Feedrate in a Face Milling Operation Using a Surface Roughness Model," International Journal of Machine Tools and Manufacture, Vol. 41, No. 3, pp. 451-462, 2001.

20. Altintas, Y., "Manufacturing Automation: Metal Cutting Mechanics, Machine Tool Vibrations, and CNC Design," Cambridge University Press, pp. 8-47, 2000.

21. Budak, E., Altinta, Y., and Armarego, E., "Prediction of Milling Force Coefficients from Orthogonal Cutting Data," Journal of Manufacturing Science and Engineering, Vol. 118, No. 2, pp. 216-224, 1996.

22. Lamikiz, A., de Lacalle, L. L., Sanchez, J., and Salgado, M., "Cutting Force Estimation in Sculptured Surface Milling," International Journal of Machine Tools and Manufacture, Vol. 44, No. 14, pp. 1511-1526, 2004.

23. Bouzakis, K.-D., Aichouh, P., and Efstathiou, K., "Determination of the Chip Geometry, Cutting Force and Roughness in free Form Surfaces Finishing Milling, with Ball End Tools," International Journal of Machine Tools and Manufacture, Vol. 43, No. 5, pp. 499-514, 2003.

24. Karpuschewski, B., Binh, N. T., and Bello, J., "An Emperical Cutting-Force Model in High-Speed-Milling Process with Spherical Cutter," Manufacturing Engineering/ Vyrobne Inzinierstvo, Vol. 6, No. 3, pp. 5-8, 2007.

25. Lee, P. and Altintaş, Y., "Prediction of Ball-End Milling Forces from Orthogonal Cutting Data," International Journal of Machine Tools and Manufacture, Vol. 36, No. 9, pp. 1059-1072, 1996.

26. Shirase, K. and Altintaş, Y., "Cutting Force and Dimensional Surface Error Generation in Peripheral Milling with Variable Pitch Helical End Mills," International Journal of Machine Tools and Manufacture, Vol. 36, No. 5, pp. 567-584, 1996.

27. Cheng, K., "Machining Dynamics: Fundamentals, Applications and Practices," Springer Science & Business Media, pp. 21-30, 2008.

28. Hu, T., "Energy Consumption Characteristics of Feed Drive System in CNC Machine Tools," Chongqing University, pp. 17-30, 2012.

29. Hu, S., Liu, F., He, Y., and Peng, B., "Characteristics of Additional Load Losses of Spindle System of Machine Tools," Journal of Advanced Mechanical Design, Systems, and Manufacturing, Vol. 4, No. 7, pp. 1221-1233, 2010.

30. Luan, X., Zhang, S., and Cai, G., "Optimal Cutting Parameters to Reduce Power Consumption in Face Milling of a Cast Iron Alloy for Environmental Sustainability," Sustainable Design and Manufacturing, pp. 135-148, 2016.